Computers and Geotechnics 36 (2009) 837–850

Contents lists available at ScienceDirect

Computers and Geotechnics

journal homepage: www.elsevier.com/locate/compgeo

Numerical modelling of soil nails in loose fill slope under surcharge loading

Y.D. Zhou, C.Y. Cheuk *, L.G. Tham

Department of Civil Engineering, The University of Hong Kong, Pokfulam Road, Hong Kong, China

ARTICLE INFO

Article history:
Received 5 June 2008
Received in revised form 13 January 2009
Accepted 20 January 2009
Available online 14 March 2009

Keywords:
Loose fill slope
Field test
Soil nail
Finite element modelling

ABSTRACT

A plane–strain numerical model has been developed to mimic a nailed loose fill slope under surcharge loading. The model has been used to back-analyse a field test that was conducted to examine the behaviour of soil nails in loose fill slopes under surcharge loading. Incremental elasto-plastic analyses coupled with pore water diffusion have been performed to study the internal deformation, water content redistribution in the soil, and the performance of the soil nails during and after the application of surcharge loading. The model parameters describing the mechanical and hydraulic properties of the nailed slope were obtained from field or laboratory tests. Different modelling techniques and boundary conditions for mimicking soil–nail interaction in loose fill material have been examined. Comparisons between numerical predictions and field measurements demonstrate that a new interfacial model, denoted as the embedded bond–slip interface model, is more suitable for mimicking the interfacial behaviour. Despite the simplicity of the numerical model, the predicted responses are in close agreement with the field test results, in particular the mobilisation and distribution of nail forces in response to surcharge loading. Both the numerical and the field test results suggest that soil nails are capable of increasing the overall stability of a loose fill slope for the loading conditions considered in this study. The increase in confining stress along the soil nails near the surcharge area is central to the overall stabilising mechanism. On the contrary, the nail forces mobilised near the nail heads are much smaller, indicating that the beneficial effect of having a structural grillage system at the slope face is limited for the range of surcharge pressures considered in this study.

1. Background

Failures of loose fill slopes have caused severe loss of lives and property in Hong Kong. These old loose fill slopes were formed in the early 1970′s prior to the establishment of the Geotechnical Control Office (now the Geotechnical Engineering Office). At that time, earthwork construction in Hong Kong was not subject to any regulatory geotechnical control. No proper compaction to a desired density was carried out when these fill slopes were constructed. As such, the fill materials, usually completely decomposed granite or volcanic soil, are in a loose state and are prone to shear failure under extreme loading events, such as heavy rainfall. Yim and Siu [1] and Wong et al. [2] have discussed the most common failure modes of loose fill slopes which include static liquefaction, sliding and washout. The current practice for upgrading existing loose fill slopes in Hong Kong consists of excavating the top 3 m of the loose fill and re-compacting the new filling material to an adequate standard, together with the provision of a drainage blanket at the base of the compacted fill. This approach has proved successful for many existing large fill slopes. However, due to the heavy machinery required for the re-compaction work, this procedure may be extremely difficult to be applied and it can be dangerous during upgrading in many heavily populated areas in Hong Kong.

An alternative method for upgrading substandard loose fill slopes is to use soil nails. The technique of soil nailing has been a very popular option for upgrading slopes in Hong Kong. However their applications have been confined to cut slopes which are formed from in-situ decomposed soils. The suitability of soil nailing in loose cohesionless fill material has been a controversial issue due to the contractive tendency of the soil when sheared. Based on a preliminary feasibility study, a design approach for soil nails in loose fill slopes has been suggested [3]. The proposed design procedure conservatively assumes that the loose fill material will soften to its steady state (or critical state) undrained shear strength when slope movements are triggered by intense rainfall. Using these conservative strength parameters, the required soil forces calculated using conventional slope stability calculations are generally very large. In addition, tie beams connecting the nail heads or a similar structural facing will be required. Although this design philosophy has been applied to upgrade existing loose fill slopes [4,5], the mechanical behaviour of soil nails in the loose fill material remains unclear. Further investigation is needed for improving the design approach.

* Corresponding author. Tel.: +852 2859 1974; fax: +852 2559 5337.
E-mail addresses: yuande@hkucc.hku.hk (Y.D. Zhou), cycheuk@hkucc.hku.hk (C.Y. Cheuk), hrectlg@hkucc.hku.hk (L.G. Tham).

0266-352X/$ - see front matter © 2009 Elsevier Ltd. All rights reserved.
doi:10.1016/j.compgeo.2009.01.010

Although many references can be found in the literature with regard to the performance of soil nails in different types of slopes [6–10], very limited work has been devoted to the complex behaviour of nailed loose fill slopes. An exception is the work by Cheuk et al. [11] who carried out numerical experiments using the finite difference programme FLAC to simulate the behaviour of nailed loose fill slope under rainfall infiltration. A soil model capable of mimicking static liquefaction was employed to examine the possible failure mechanisms. The numerical simulations suggested that a nailed slope without a facing structure behaved similarly to a loose fill slope without soil nails due to the low residual shear resistance along the soil–nail interface when the soil was "liquefied". Although the assumption that the soil would soften to its critical state undrained shear strength is a conservative one, the conclusion drawn from the study has formed the basis of the design approach currently adopted in Hong Kong [3]. Li [12] reported a field test in which the performance of soil nails installed in a purposely-built loose fill slope was investigated. A number of different loading conditions, such as surcharge and water infiltration, were considered. The soil nails were observed to provide a global stabilising effect. The nail force distributions, the slope movements and the change in water content distributions were recorded.

This paper describes a two-dimensional plane–strain numerical model for the investigation of the behaviour of soil nails in loose fill slopes. A series of elasto-plastic analyses coupled with pore water diffusion have been conducted to back-analyse the field test described in Li [12]. The focus is placed on the surcharge process in which significant nail forces are mobilised in the soil nails. Two modelling techniques for mimicking the interfacial behaviour at the soil–nail interface have been considered. Different boundary

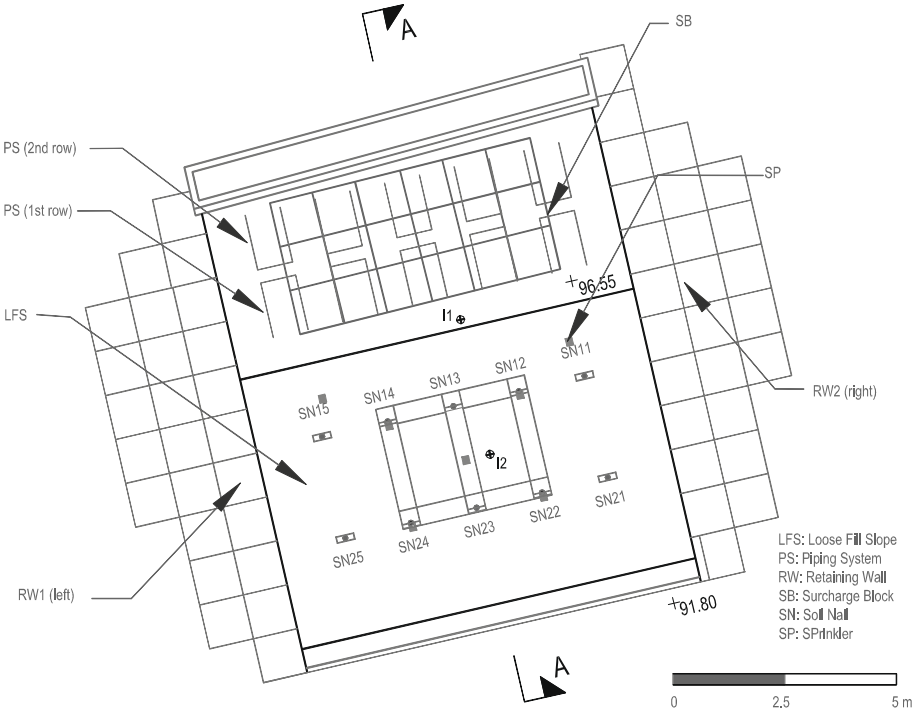

(a) Plan view

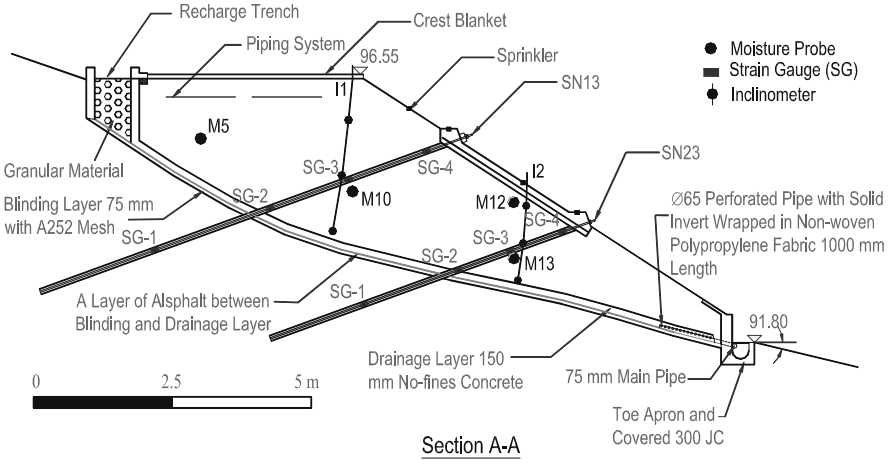

(b) Section view

Fig. 1. General arrangement of the field test.

conditions at the nail ends have also been examined. The numerical results are compared with the field monitoring data to assess the adequacy of each modelling approach. Using the most appropriate modelling approach, together with the field observations, the mechanism of nail force mobilisation has been studied.

2. Brief description of the field test

2.1. Construction of the test slope

The field test was conducted on a purposely-built loose fill slope (Fig. 1) constructed by end-tipping completely decomposed granite (CDG) on a selected site, which is moderately gentle with an average gradient of 20°. The 4.75 m high fill slope had an inclination angle of 33°, which is the average slope angle of most fill slopes in Hong Kong [13]. The total width of the slope was 9 m, with a crest area of 4 m long. The initial degree of compaction of the loose fill prior to the field test was ~75% of the maximum dry density measured in a standard Proctor test, and the initial moisture content of the soil was 14.9%. As shown in Fig. 1, two gravity retaining walls were constructed on both sides to laterally confine the loose fill slope, and a 0.8 m high toe apron was built at the toe of the slope. A blinding layer, which is made up of ordinary concrete and reinforced by A252 steel mesh, and a layer of no-fines concrete was placed underneath the fill to isolate it from the in-situ ground, and to provide a drainage path for water infiltration during the second stage (i.e. wetting) of the field test.

As shown in Fig. 1, ten numbers of grouted nails divided into two rows were installed at vertical and horizontal spacings of 1.5 m. The inclination of the nails was 20° to the horizontal. The construction procedures were similar to those commonly adopted in Hong Kong. A 100 mm diameter hole was first drilled, and a 25 mm diameter steel ribbed bar was then inserted into the hole with centralizers to fix the position. Finally, the hole was filled with ordinary cement grout. Two types of nail heads were adopted in the field tests, namely independent head and grillage beams, as shown in Figs. 1 and 2.

2.2. Field test programme

The entire field test was divided into three stages, namely (1) surcharge only, (2) wetting with surcharge, and (3) wetting without surcharge. In this paper, the main attention is placed on the performance of the slope during the surcharge process in which nail force mobilisation is most significant. The surcharge pressure, originated from the self-weight of concrete blocks, was applied sequentially onto the slope crest in four stages and the final total surcharge pressure was 72 kPa. A comprehensive instrumentation system, including inclinometers, moisture probes, tensiometers and strain gauges, was installed in the slope. The data have been used to evaluate the different numerical modelling approaches considered in this study. Further information of the field test can be found in Li [12].

3. Details of the numerical model

3.1. Basic assumptions

During the surcharge stage of the field test, the loose fill remained unsaturated. The contribution of the suction to both the shear strength and the volumetric behaviour of the soil may affect the overall response of the nailed slope, and therefore needs to be taken into account in the numerical model. In this study, the loose fill is treated as a porous medium and modelled by the conventional approach that considers soil as a multiphase material and adopts the effective stress principle to describe its mechanical behaviour. The finite element package ABAQUS is used as a platform for the analyses [14].

The elementary volume of the soil, dV, is made up of two components: (1) incompressible soil grains, dV_g, and (2) voids which are filled by either air or water, dV_v (i.e., $dV = dV_g + dV_v$). The amount of pore water, which is free to flow through the soil skeleton, is denoted as dV_w, while $dV_w \leqslant dV_v$. It is assumed that the loose fill is permeable enough for air flow to be connected to the atmosphere such that pore air pressure is always zero. This is a common assumption for slope analyses concerning unsaturated soils at shallow depths. A simplified effective stress principle has been adopted:

$$\bar{\boldsymbol{\sigma}} = \boldsymbol{\sigma} - \chi(s) u_w \mathbf{I} \tag{1}$$

where $\bar{\boldsymbol{\sigma}}$ and $\boldsymbol{\sigma}$ are the effective and total stresses respectively; u_w denotes the pore water pressure; χ is a factor that depends on the saturation degree s, and $\mathbf{I}$ is a second-order unit tensor. The χ function is assumed to be equal to the saturation degree of the soil for simplicity (i.e., $\chi = s$).

Fig. 2. View of finished soil nailed loose fill slope (with surcharge).

3.2. Governing equations

The fundamental equations describing stress equilibrium of the soil skeleton and flow continuity of pore water are given as follows:

$$\int_V (\bar{\boldsymbol{\sigma}} + \chi u_w \mathbf{I}) : \delta\boldsymbol{\varepsilon} dV = \int_s \mathbf{t} \cdot \delta\mathbf{v} dS + \int_V \mathbf{f} \cdot \delta\mathbf{v} dV + \int_V sn\rho_w \mathbf{g} \cdot \delta\mathbf{v} dV \tag{2}$$

$$\frac{d}{dt}\left(\int_V \frac{\rho_w}{\rho_w^0} sn dV\right) = -\int_s \frac{\rho_w}{\rho_w^0} sn\mathbf{n} \cdot \mathbf{v}_w dS \tag{3}$$

where $\delta\boldsymbol{\varepsilon} = sym(\partial\delta\mathbf{v}/\partial\mathbf{x})$ denotes the virtual rate of deformation; $\delta\mathbf{v}$ is a virtual velocity field; $\mathbf{t}$ are surface tractions per unit area; $\mathbf{f}$ are body forces (excluding pore water weight) per unit volume; n is the porosity of the soil; ρ_w is the water density, and $\mathbf{g}$ is the gravitational acceleration; $\mathbf{v}_w$ is the seepage velocity; $\mathbf{n}$ is the outward normal to S; ρ_w^0 is the reference density of pore water for normalisation of the flow continuity equation.

Darcy's Law is adopted to simulate the pore fluid flow within the soil, which has been shown to be valid for unsaturated soils if the coefficient of permeability, k, is written as a function of the degree of saturation, s:

$$sn\mathbf{v}_w = -\mathbf{k}(s) \cdot \frac{\partial h}{\partial \mathbf{x}} \tag{4}$$

where h is the piezometer head, defined as $h = z + \frac{u_w}{\rho_w g}$, in which z is the elevation above an arbitrary datum and g is the gravitational acceleration.

3.3. Solution algorithm

As the behaviour of unsaturated soil is strongly coupled with pore fluid flow, the stress equilibrium and flow continuity equations are solved simultaneously. The stress equilibrium equation is discretised using a Lagrangian formulation for the soil skeleton, with displacements being taken as nodal variables, whilst the continuity equation is integrated in time using the backward Euler approximation method discretised with finite elements using pore water pressure as a field variable. It is in general a nonlinear case when the seepage and mechanical behaviour are coupled in the system equations. The Newton–Raphson method is used to calculate the incremental numerical solutions.

3.4. The finite element mesh and boundary conditions

The finite element mesh is set up according to the geometry of the middle section of the slope. It is believed that mobilisation of nail forces along this section was most effective in the field test due to the presence of a surface grid structure. As shown in Fig. 3, the slope is modelled using a finite element mesh consisting of 1142 plane–strain four-node bilinear elements. Each node has three degrees of freedom, one for pore water pressure and two for displacements. Considering that a layer of asphalt was applied above the natural ground surface as a watertight measure in the field test and that redistribution of water content within the in-situ ground underneath the fill was negligible, only deformations were taken as the field variables for the in-situ ground in the numerical model. The drainage layer (i.e. no-fines concrete layer) is also modelled as a deformable porous medium by finite elements with coupled nodal variables.

The displacement boundary conditions of the numerical model are taken as vertical rollers on the left boundary, and full fixity at the base and the constrained region at the concrete apron near the toe. Since no water could flow out from the unsaturated slope during the surcharge process, no-flow conditions are assumed along the outer boundary of the entire model. Moreover, the interfaces between the no-fines concrete layer and the surrounding

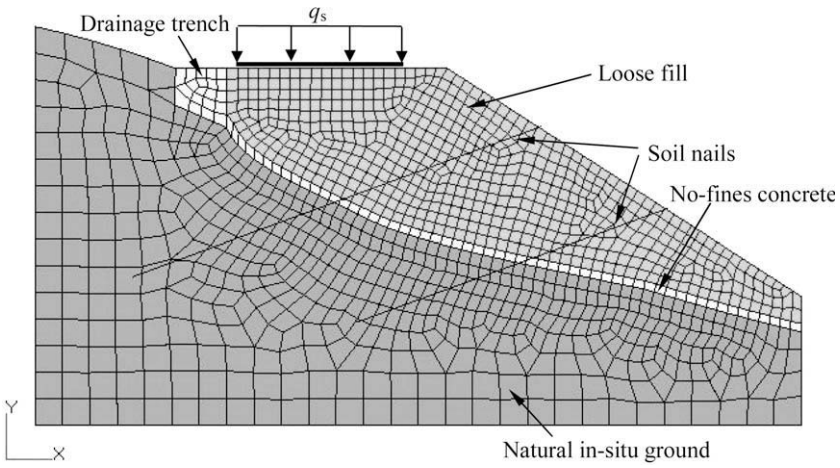

Fig. 3. Finite element model of the nailed loose fill slope.

Table 1
Summary of material parameters.

	Initial conditions	Elastic property	Shear strength	Hydraulic property
CDG loose fill	γ_d = 1.41 *kg* /m3, e_0 = 0.86, M_{c0} = 14.9%	μ = 0.05, κ = 0.011	c' = kPa, φ' = 32°, ψ = 5°	k – Fig. 5 SWCC – Fig. 6
Soil nails	–	$E = 2.5 \times 10^4$ MPa, μ = 0.2	–	–
In-situ ground	–	E = 35 MPa, μ = 0.25	–	–
No-fines concrete	–	$E = 1 \times 10^4$ MPa, μ = 0.2	–	$k = 1.0 \times 10^{-4}$ m/s
Soil–nail interface	–	E= 10 MPa, μ = 0.2	c' = 10.6 kPa, φ' = 35.8°	–

Note: E, μ, κ, M_{c0}, γ_d, e_0, k, $c'$and φ' are Young's modulus, Poisson's ratio, the slope of the unloading–reloading line on the $v - \ln p'$ diagram, initial moisture content, dry density, initial void ratio, permeability coefficient, cohesion intercept and internal friction angle respectively, and the subscript "0" denotes the initial value.

soils are assumed to be continuous with no slippage allowed as a deep-seated failure mechanism along the interfaces was not observed in the field test.

The average void ratio and degree of saturation of the soil measured prior to the field test have been adopted as the initial conditions for the analyses (Table 1). The initial distributions of internal stresses and pore water pressures within the slope under the gravity loads are then obtained by initial equilibrium calculations before surcharge loading is imposed on the slope. Fig. 4 shows the sequence of the surcharge pressure applied to the slope during the field test. The surcharge is modelled by a uniform pressure applied to crest area of the slope (Fig. 3).

3.5. Soil models and parameters

The loose CDG forming the fill slope is modelled by the Mohr–Coulomb (M–C) plasticity model with a non-associated flow rule. To capture the stress-dependent stiffness of typical residual soils, the bulk modulus, K, of the soil skeleton is written as a function of the mean effective stress, p', according to

$$K = \frac{\partial p'}{\partial \varepsilon_v^e} = \frac{1+e}{\kappa} p' = \frac{v}{\kappa} p' \tag{5}$$

where ε_v^e denotes the elastic volumetric strain, e is the void ratio, $v = 1 + e$ is the specific volume, and κ is the slope of the recompression-unloading line on the $v - \ln p'$ diagram. The Poisson's ratio, μ, is assumed to be a constant and the shear modulus, G, is given by:

$$G = \frac{3(1-2\mu)vp'}{2(1+\mu)\kappa} \tag{6}$$

Fredlund et al. [15] proposed a modified M–C failure criterion, in which two friction angles, ϕ' and ϕ^b, are used to quantify the contribution of net normal stress and matric suction to shear resistance respectively. For residual soils in Hong Kong, the value of ϕ^b is usually equal to or less than ϕ' [16]. The two angles are assumed to be the same in this study such that the shear strength of the soil is given by:

$$\tau = c' + (\sigma - s \cdot u_w) \tan \phi' \tag{7}$$

A smooth flow potential function proposed by Menétrey and Willam [17] is adopted in the model. The function has a hyperbolic shape in the meridional stress plane and a piecewise elliptic shape in the deviatoric stress plane. Plastic flows in the deviatoric and meridional planes are non-associated in general, and dilatancy can be controlled by the dilation angle. A perfect plastic hardening law is assumed in the calculations. Table 1 summarises the model parameters adopted in the analyses. The stiffness and strength parameters are derived from relevant experiments [12]. The angle of dilation, ψ, is taken as a small value of 5° to allow minimal shear-induced volumetric expansion in the loose fill material.

The hydraulic behaviour of the unsaturated soil is governed by the permeability function and the soil–water characteristic curve (SWCC). Based on the observations from laboratory tests and field measurements, a simplified piecewise permeability function for the loose CDG fill is defined as shown in Fig. 5a. Fig. 5b presents the SWCC adopted in the analysis, which approximates the measured SWCCs obtained from field wetting tests.

For the natural ground and the no-fines concrete layer underneath the loose fill, the deformation is small enough that they can be modelled by a linear elastic model with the model parameters listed in Table 1. The coefficient of permeability, k, of the no-fines concrete layer is taken as 10^{-4} m/s to represent its free-draining property.

3.6. Modelling of soil nails

Each soil nail is made up of a steel rod and grout, and is idealised as a one-dimensional elastic homogeneous bar in the numerical model as the possibility of yielding is fairly low. With the introduction of the compatibility assumption of axial deformation between the grout and the steel rod along the nailing direction, the equivalent Young's modulus of the idealised bar is determined as follows:

$$\tilde{E} = \frac{E_r A_r + E_g A_g}{A_r + A_g} \tag{8}$$

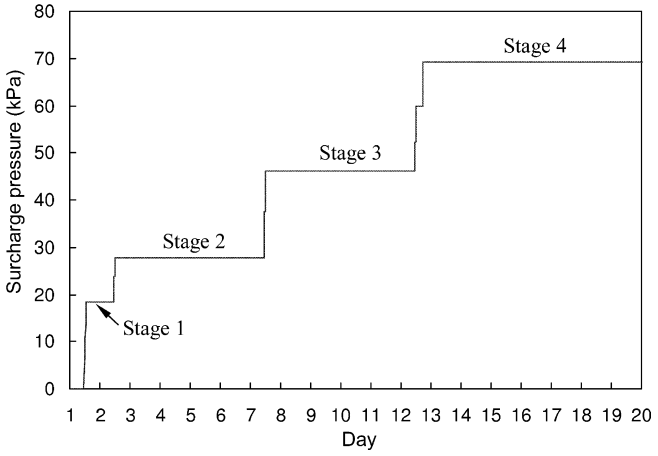

Fig. 4. Change in surcharge pressure during the field test.

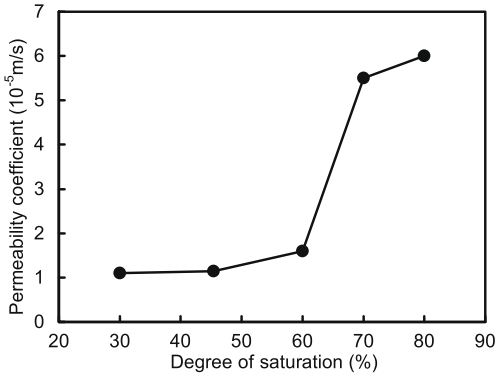

(a) Permeability coefficient versus degree of saturation

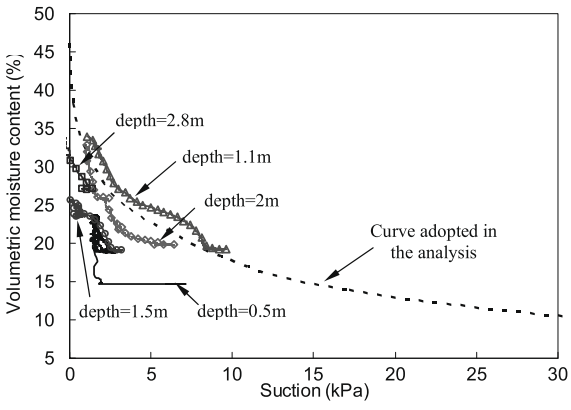

(b) Water retention curve (solid lines denote field measurements)

Fig. 5. Hydraulic properties of the CDG loose fill.

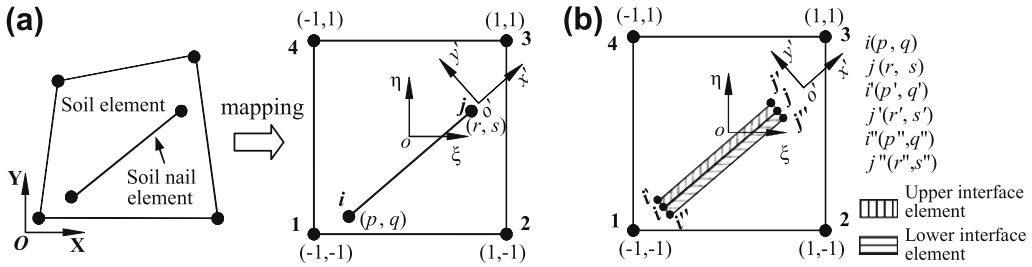

Fig. 6. Modelling of nail–soil interface (a) embedded element model (b) embedded bond–slip model.

Table 2
Summary of the analyses.

Cases	Soil nails	Interfacial model	Fixed displacement at nail end	Grillage system
1	Yes	Embedded element	No	No
2	Yes	Bond–slip	No	Yes
3	Yes	Bond–slip	No	No
4	Yes	Bond–slip	Yes	No
5	No	–	–	–

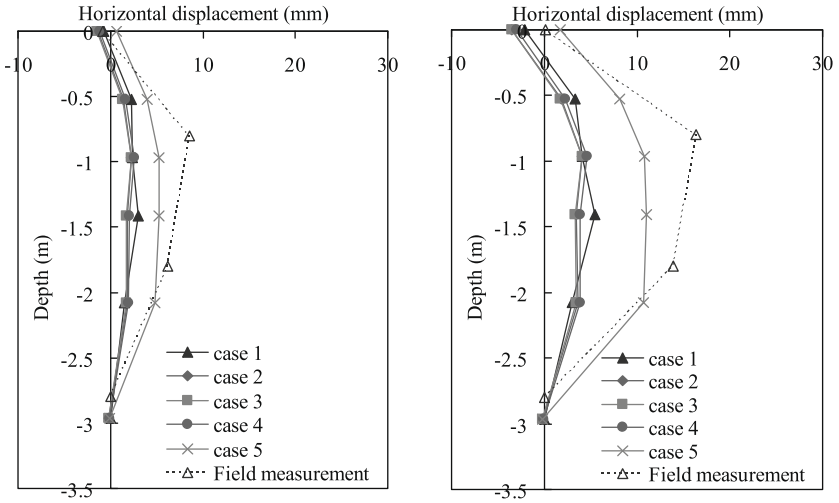

(a) at the end of stage 2 (q_s=30kPa) (b) at the end of stage 3 (q_s=49kPa)

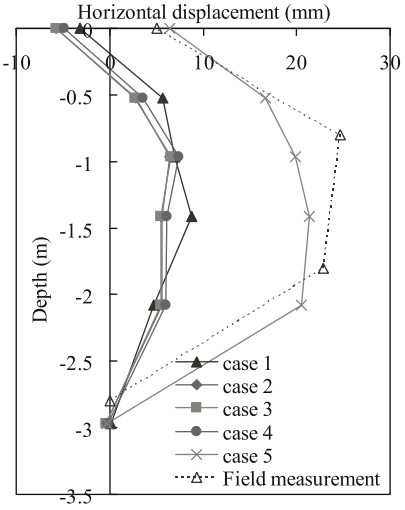

(c) at the end of stage 4 (q_s=72kPa)

Fig. 7. Variation of horizontal displacement at I1 at different surcharge stages.

where $\tilde{E}$ is the equivalent elastic modulus of soil nail, $E_r(A_r)$ and $E_g(A_g)$ are the elastic modulus (equivalent cross-sectional area) of the steel rod and the grout, respectively. The equivalent cross-sectional areas of the steel rod and the grout are calculated based on a unit width of the nailed slope in order to take into account the horizontal spacing in the plane–strain model.

The modelling approach for the interaction between the soil nail and the surrounding soil has a direct impact on the global behaviour of the nailed slope. Different strategies have been considered in this study to identify the most appropriate approach through comparisons between numerical predictions and field test results. For the interaction along the soil–nail interface, two approaches denoted as "embedded element technique" and "embedded bond-slip interface model" are considered. Details of these approaches are described below.

3.6.1. Embedded element technique

The embedded element technique is a conventional approach available in ABAQUS [14], which has been widely used in numerical analyses of reinforced concrete structures, for example Kwak and Filippou [18]. In this approach, perfect bonding between the nail and the surrounding soil is assumed. It therefore implies full compatibility between the soil nail and surrounding soil (i.e. no slippage). This technique models the reinforcements through embedding an element or a group of elements in the "host" elements as illustrated in Fig. 6a. According to the geometric relationships between the nodes of the embedded elements and those of the host elements, the displacements of the embedded nodes are interpolated from the displacements of the hosts' nodes. Detailed descriptions of the technique can be found in [18].

3.6.2. Embedded bond-slip interface model

The embedded bond-slip interface model is a new model developed for this study. The model combines the characteristics of the embedded element technique described above and the interface element method, which was originally proposed to model nonlinear behaviour of rock joints by Goodman et al. [19]. As depicted in Fig. 6(b), the entire nail-grout composite is represented by a bar element (element ij) sandwiched between a pair of four-node plane interface elements (elements $ijj'i'$ and $ijj''i''$). The nodal displacements at the edges $j'i'$ and $j''i''$ are determined by the geometric relationships between the nodes and the nodal displacements of the host soil element, as in the embedded element technique. The axial deformation of the bar element dictates the nail force developed, whilst the relative shear deformations of the interface elements determines the traction exerted along the soil–nail interface. The constitutive relationship for the soil–nail interface elements can be directly specified in terms of a traction–separation

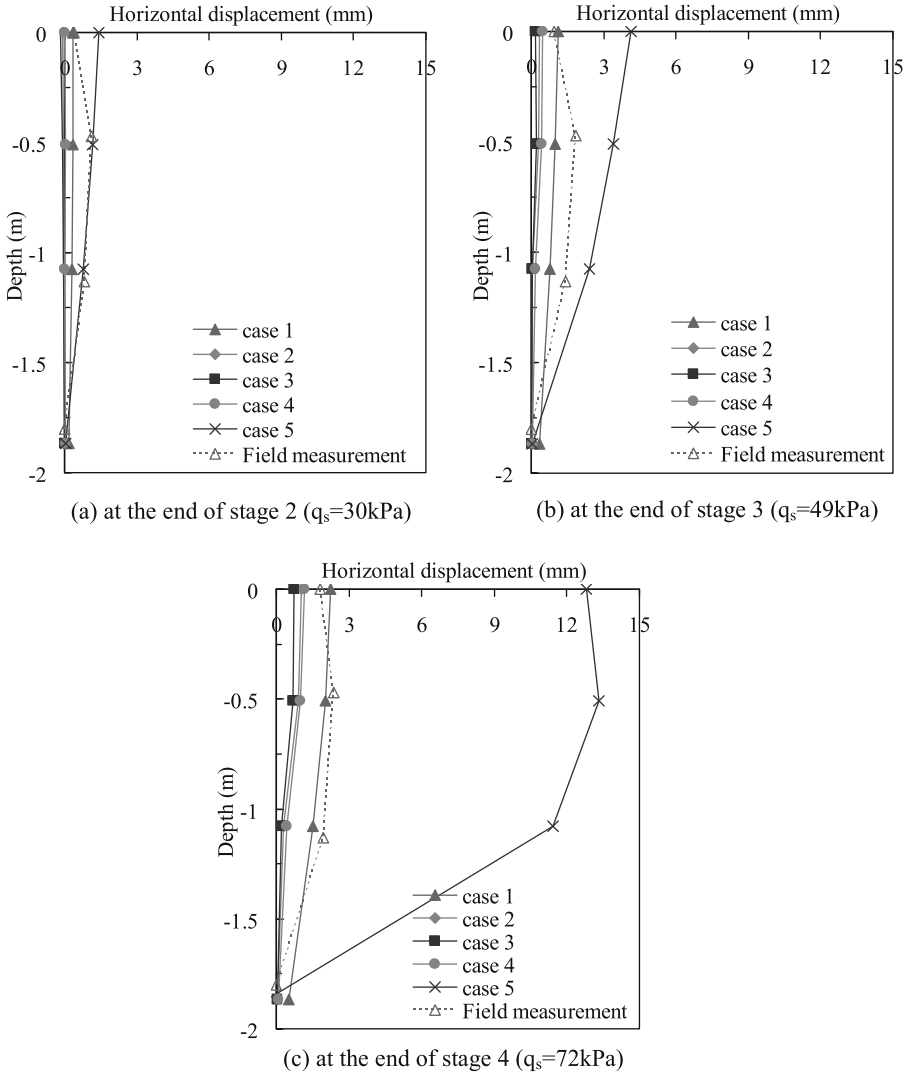

Fig. 8. Variation of horizontal displacement at I2 at different surcharge stages.

relationship, or defined based on a continuum-based material model with only the through-thickness direct strain and the transverse shear strain components incorporated. In this paper, the latter approach is adopted and the elastic behaviour is controlled by the Young's modulus and Poisson's ratio of an assumed interface layer, whilst the limiting frictional resistance (τ_n) is given by:

$$\tau_n = c_n + \sigma'_n \tan \phi_n \tag{9}$$

where c_n is an equivalent cohesion parameter for the soil–nail interface; φ_n is the corresponding friction coefficient, and σ'_n is the effective normal stress exerted on the interface.

To evaluate the frictional characteristics of the soil–nail interface, four pullout tests were carried out prior to the field tests. The pullout resistance is linked to the average overburden pressure exerted on the soil nail. This gives the apparent cohesion intercept and equivalent friction coefficient of 10.6 kPa and 0.72 (35.8°), respectively. It should be noted that the nail–soil interface strength parameters are higher than the strength parameters of the fill. This could be due to many possible reasons, such as constrained dilation as the nail force is mobilised, over-break in the drill-hole, etc. Nonetheless the measured coefficients are still relatively low as compared to test data on other types of nailed slopes (e.g. [20,21]), presumably due to the loose nature of the fill material. Details of the embedded bond–slip interface model and numerical verifications can be found in [22]. The model parameters adopted for the embedded bond–slip interface model are given in Table 1.

In addition to the interfacial behaviour along the soil–nail interface, the boundary conditions at the two ends of a nail also have direct impact on the nail force mobilisation. There are two different options for the end condition at the end tip (i.e. the embedded end); this can be either a free displacement condition or a full fixity. Both two options have been examined to evaluate the nail response. For the constraint at the slope surface, a free end condition represents a soil nail without any nail head or facing structure. Alternatively, the "nail heads" are connected together using an independent bar element to simulate the grillage effect at the slope surface. The bar elements, with a specified elastic stiffness, merely connect the node points together and no interaction between the grid structure and the soil has been considered.

It should be emphasised that soil nails are modelled as two-dimensional flat plates of equivalent cross-sectional area and stiffness in this study. The plane–strain simplification ignores the three-dimensional geometry of the soil nails and is considered appropriate only if the overall behaviour of the nailed slope is of concern.

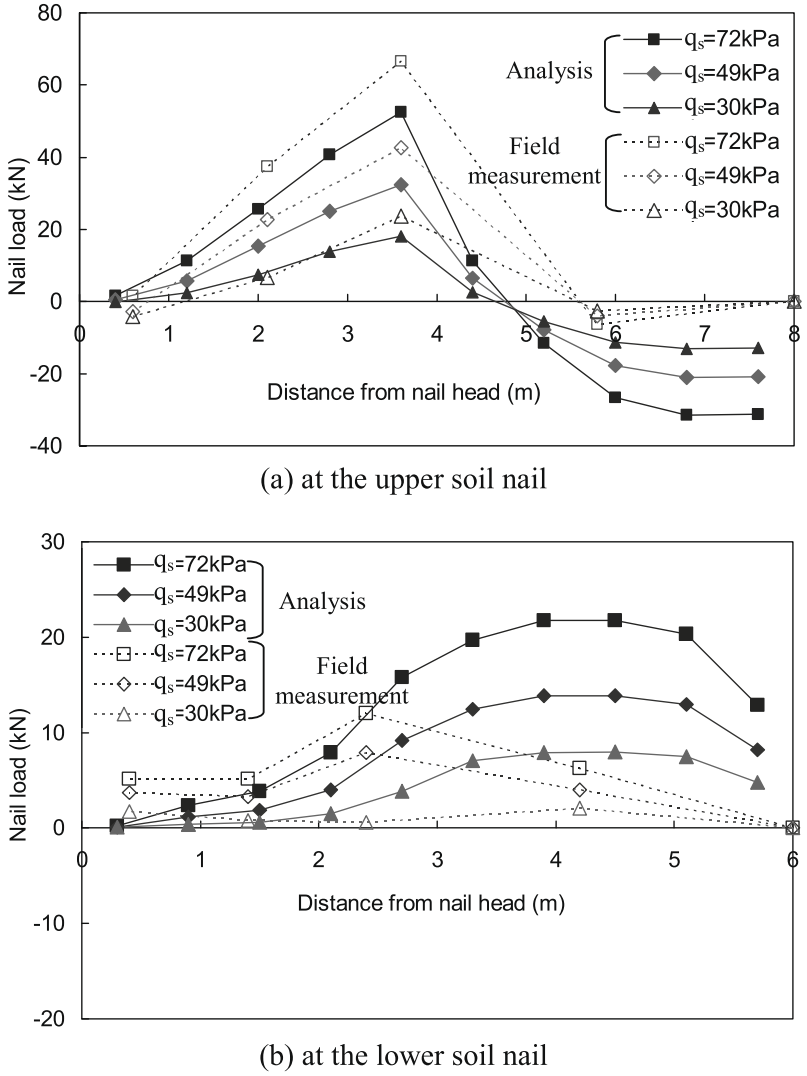

Fig. 9. Distribution of nail loads during the surcharge process (case 1: embedded element model, no grillage, no anchor at the nail ends).

3.7. Analysis programme

A total of five analyses have been conducted in this study. The analysis conditions are tabulated in Table 2. All the analyses are all fully coupled with the sequence of the surcharge loading simulated on a real time scale over a period of ~20 days (see Fig. 4). Different combinations of modelling techniques and considerations have been examined to identify the most appropriate approach for modelling nailed loose fill slopes. A hypothetical case of a loose fill slope without soil nail has also been considered to illustrate the failure mechanism of an un-reinforced model slope. This benchmark analysis is used as a basis of comparison to examine the stabilising mechanisms of soil nails in loose fill slopes.

4. Results and discussions

4.1. Deformation patterns

Two inclinometers were installed in the slope near the central section, denoted as I1 for the one at 300 mm from the slope crest and I2 for the one installed in the middle (Fig. 1). The horizontal displacements in the down-slope direction were monitored by the three sensors installed on each inclinometer during the field test. Figs. 7 and 8 compare the predicted and measured horizontal displacements at the two inclinometer positions at different surcharge stages. The predictions for an un-reinforced slope (i.e. case 5) are also shown for comparison. The four nailed slope models with different modelling approaches give very similar deformation patterns, which are also similar to that observed in the field test, except that the magnitude of the predicted movements are smaller. The relatively small soil movements predicted by the numerical model can be mainly attributed to the 2D simplifications made in the model. The inclinometers were installed at 0.5 m away from the central section where nail reinforcements are located (Fig. 1). The local strengthening effect may cause the soil near the inclinometers to deform more than that near the soil nails. In addition, the simple nature of Mohr–Coulomb shear failure criterion, which cannot capture any plastic deformation induced by a significant increase in mean confining pressure due to the surcharge, may also have contributed to the smaller predicted deformations.

Comparing the two inclinometers, larger soil deformations are mobilised at I1. This can be attributed to the fact that it is in the immediate vicinity of the surcharge area. Both the simulation and the field test demonstrate that considerable horizontal displacements are mobilised at a depth of ~1.5 m below the ground surface at I1 as the surcharge pressure increases. This implies that a bulge-shaped mechanism similar to a bearing capacity failure is developed in the region beneath the slope crest. This may indicate

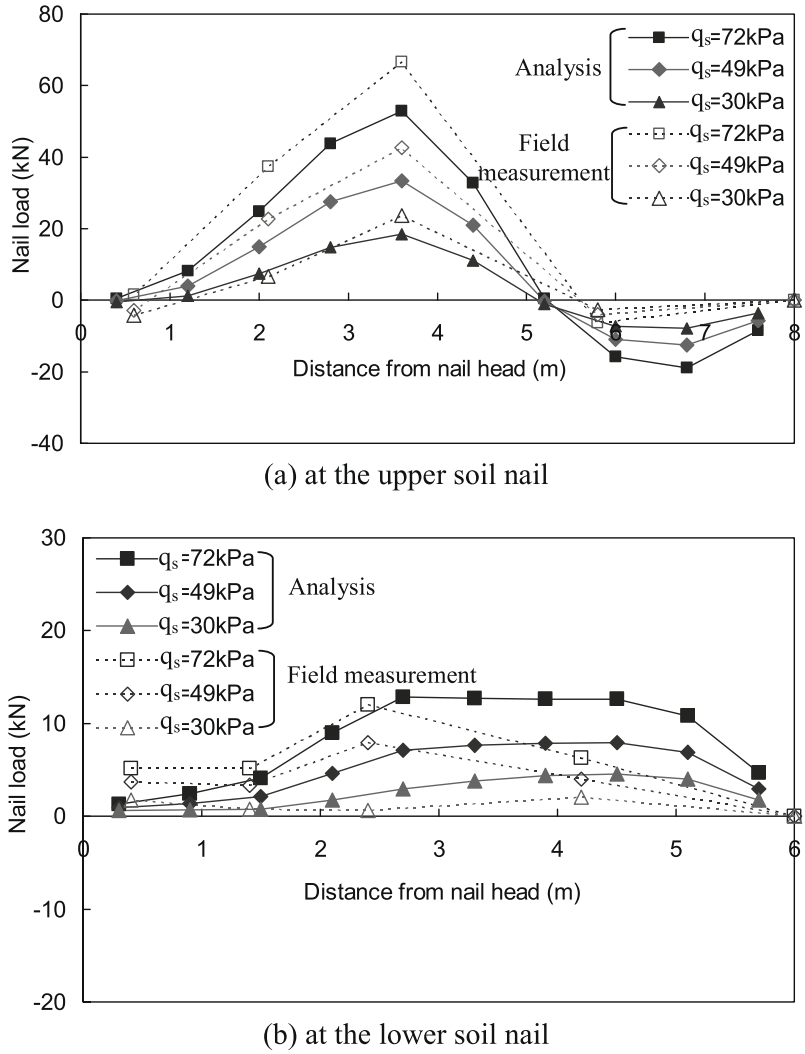

Fig. 10. Distribution of nail loads during the surcharge process (case 2: embedded bond–slip model, grillage modelled, no anchor at the nail ends).

that the soil nails are providing stabilising forces to avoid the formation of a sliding mass.

Among the four slope models with nails, larger soil deformations are predicted when the embedded element technique is used to model the soil–nail interface (i.e. case 1). The difference is particularly noticeable for the displacement profile at the position of inclinometer I2, despite that the displacements are small in magnitude. A comparison among the three cases using the embedded bond–slip model (i.e. cases 2–4) reveals that the boundary conditions at the ends of the nails have very minor influence on the overall response of the slope as far as deformation pattern is concerned. This observation highlights that the soil–nail interface model is of primary importance if good predictions of the overall response are to be achieved by numerical modelling.

4.2. Nail force distribution

Figs. 9–12 compare the calculated nail forces with the field measurements. Each figure corresponds to each of the four models with different modelling approaches. The field measured nail forces were interpreted from the strain gauges installed on nails SN13 (upper) and SN23 (lower), which were both located along the central section (see Fig. 1). All the four models, despite using different modelling approaches, predict very similar nail force patterns as those observed in the field test. Particularly good agreement can be seen for the upper soil nail, whilst over-predictions to different extents are resulted for the lower soil nail depending on the modelling approach adopted. Among the four models, case 3, which models both nail ends as free nodes, gives the closest overall response. Although slightly closer predictions are obtained for the lower soil nail in case 4, in which the embedded end of the nail is fixed to model full anchorage, very significant compressive forces are calculated for the upper nail. No strain gauge was mounted on the nail along the portion buried in the in-situ ground, but the reading from the deepest strain gauge on the upper soil nail showed a compressive force of <10 kN. The very large predicted compressive forces are therefore considered to be unrealistic. The above comparisons conclude that the most appropriate approach to model soil nails in loose fill under surcharge loading is to adopt the embedded bond–slip model for the interfacial behaviour and not restricting the movement of the end nodes of the nail element.

The numerical predictions and the field monitoring data illustrate that larger nail forces are mobilised in the upper soil nail under the surcharge loading. This is consistent with the larger soil deformation (Figs. 7 and 8) which also implies larger relative movement along the soil–nail interface. In addition, the surcharge loading directly increases the normal stress exerted on the upper soil nail. The maximum normal stress acting on the upper nail rises

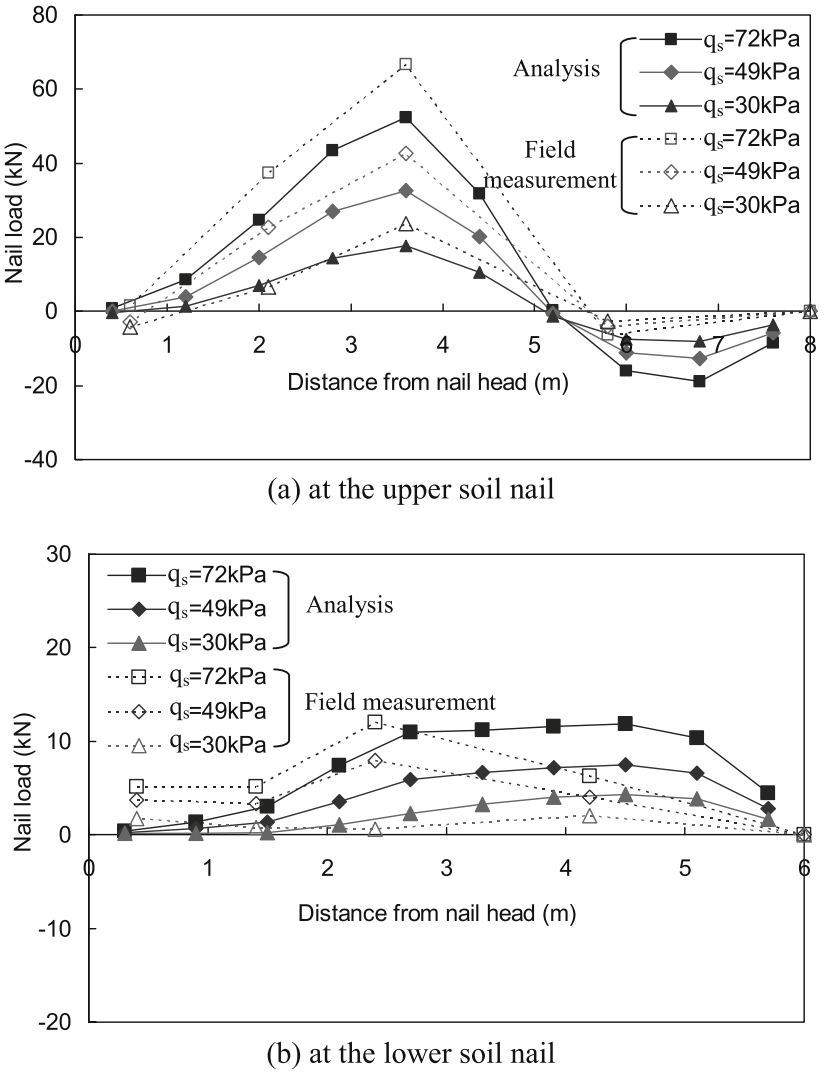

Fig. 11. Distribution of nail loads during the surcharge process (case 3: embedded bond–slip model, no grillage, no anchor at the nail ends).

from 37 to 86 kPa when the surcharge pressure increases from 0 to 72 kPa. The initial normal stress of 37 kPa originated from the overburden pressure, in which less than 4% (1.3 kPa) came from the suction component in Eq. (1), can only provide a maximum tangential resistance of 12 kN according to Eq. (9). In other words, the surcharge loading directly increases the confining stress exerted on the upper soil nail, hence the pull-out resistance of the soil nail.

Numerical simulations and field data show that the maximum nail forces are mobilised at approximately 3.5 m away from the nail heads. Although a grid structure was present in the field test, which is also modelled in the numerical analysis using a bar element, very limited tensile force (<10% of the maximum nail force) is mobilised at the nail heads. This is presumably due to the small relative movement along the soil–nail interface near the slope surface. In addition, the low confining stress near the slope surface is also a contributing factor. For example, the calculated normal stress exerted along the upper nail near the nail head is only ~7 kPa even when the surcharge load is fully applied (i.e. 72 kPa).

4.3. Moisture content distribution

Apart from the insights into the mechanical behaviour of the nailed slope, the coupled analyses can also predict the change in moisture content distribution in the soil during the surcharge process. In the field test, three moisture content probes (M10, M12 and M13 in Fig. 1) were installed near the inclinometers, whilst M5 was embedded directly underneath the surcharge area to monitor the change in water content. Although no water had entered into the slope during the surcharge process, the moisture content within the unsaturated loose fill still underwent slight redistributions when surcharge load was applied, as indicated by the moisture probe readings. These readings can be used to examine the capability of the model in predicting moisture redistribution. Fig. 13 compares the calculated and measured volumetric moisture content at the locations of the moisture probes (Fig. 1). It can be observed that good agreement is achieved between the field and numerical results, both showing a gradually decreasing trend. The difference between predictions and field measurements at moisture probes M5 and M10 is presumably caused by the different initial conditions. The initial conditions adopted in the numerical analyses are achieved by running the model to an equilibrium state. The resulted distribution of moisture content may deviate from the actual distribution measured on site. The capability of the numerical model in predicting the change in moisture content in unsaturated soil is very useful in the evaluation of slope response under water infiltration, which is discussed in [22]. For the surcharge loads considered in this

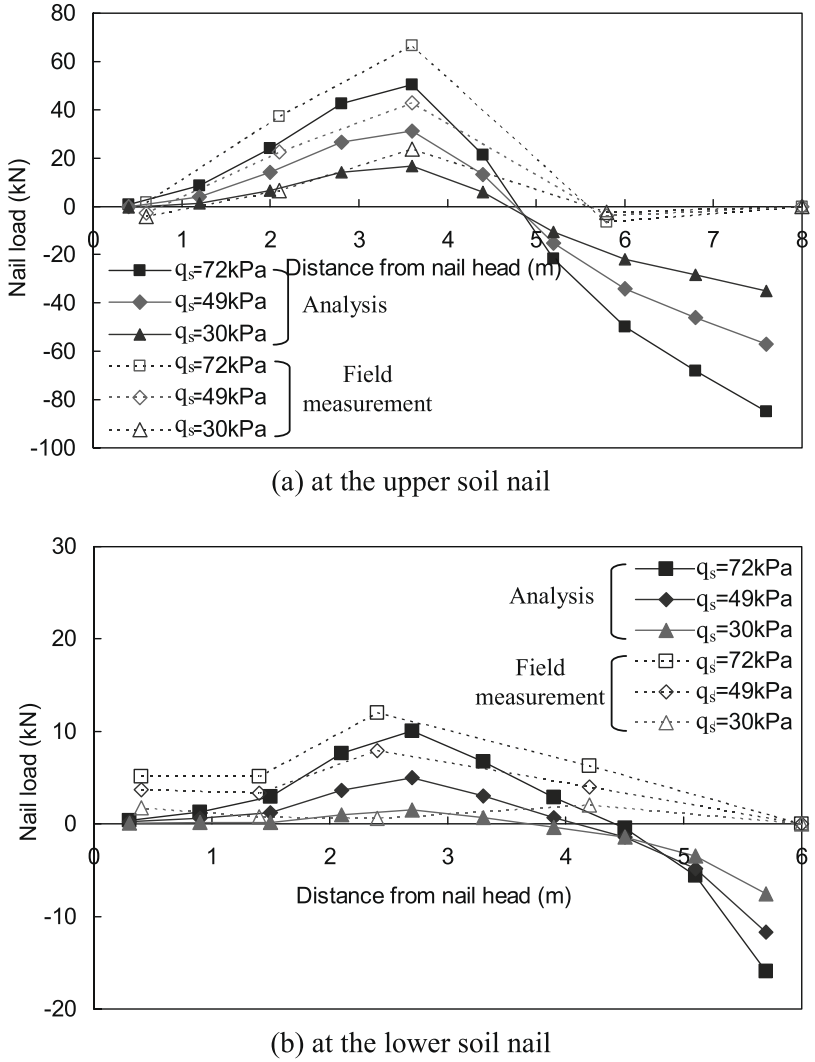

Fig. 12. Distribution of nail loads during the surcharge process (case 4: embedded bond–slip model, no grillage, full anchor at the nail ends).

paper, the influence of moisture content redistribution is believed to be negligible.

4.4. Role of soil nails in loose fill slopes

To examine the role of soil nails in loose fill slopes, the failure mechanisms of an un-reinforced (i.e. case 5) and a nailed loose fill slope triggered by extreme surcharge loading are examined. Fig. 14 compares the plastic shear strain mobilised at failure in these two cases. The modelling conditions for the nailed slope model are identical to those in case 3 (Table 2), except that the surcharge pressure is increased until global failure is triggered, which occurs at q_s = 216 kPa.

Meyerhof's bearing capacity equation predicts that failure would occur in the un-reinforced loose fill slope at a surcharge of about 119 kPa, which is close to the 138 kPa predicted by the numerical model. The failure mechanism involves a global sliding plane initiating from the crest of the slope near the surcharge area to the slope toe (Fig. 14a). The presence of the soil nails significantly increases the rigidity of the soil located below the upper soil nail. The failure mechanism of the nailed slope consists of a very localised plastic zone originated from the centre of the surcharge area (Fig. 14b). Although a zone of large plastic shear strain is also formed near the edge of the surcharge area, which is where the global failure mechanism of the un-reinforced slope is initiated, the development of this shear zone is prohibited by the upper soil nail. The corresponding nail force distributions plotted in Fig. 15 suggest that a much larger nail force is mobilised in the upper soil nail than in the lower one.

The above comparison illustrates that soil nails could significantly increase the stability of a loose fill slope under surcharge loading. The upper row of soil nails play the key role in taking up the surcharge loading, partly due to their vicinity to the applied pressure, and partly due to the enhanced pull-out resistance caused by the increase in confining stresses. The present study considers only surcharge pressure, however. The performance of the soil nails in the loose fill slope could be significantly different if the loading is triggered by rainfall infiltration. Cheuk et al. [11] conducted some numerical experiments on a loose fill slope reinforced by soil nails, in which the soil and the soil–nail interface,

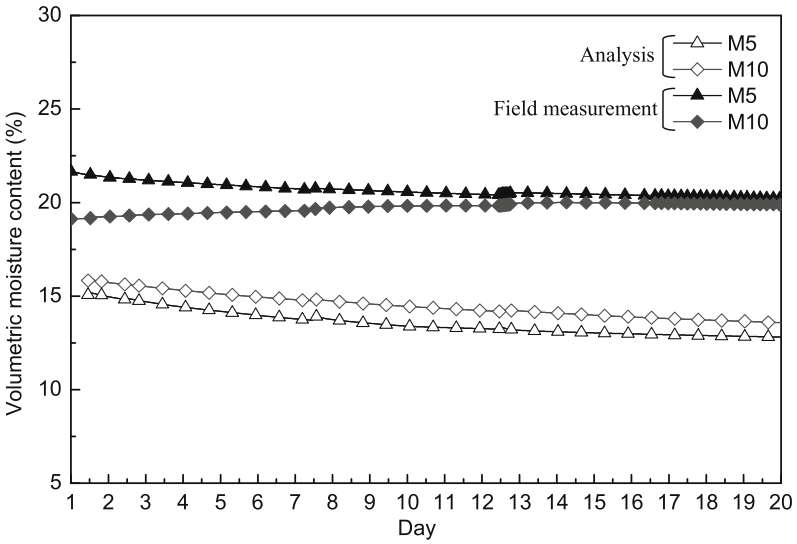

(a) at M5 and M10

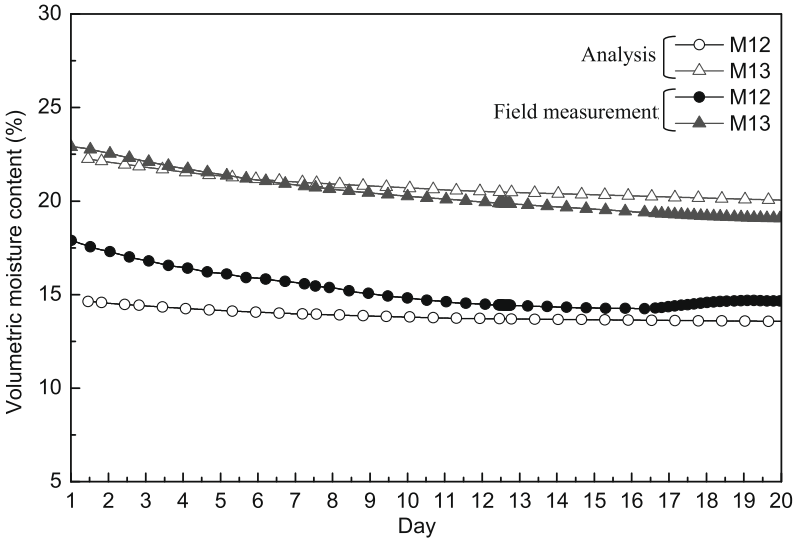

(b) at M12 and M13

Fig. 13. Variation of volumetric moisture content during the surcharge process.

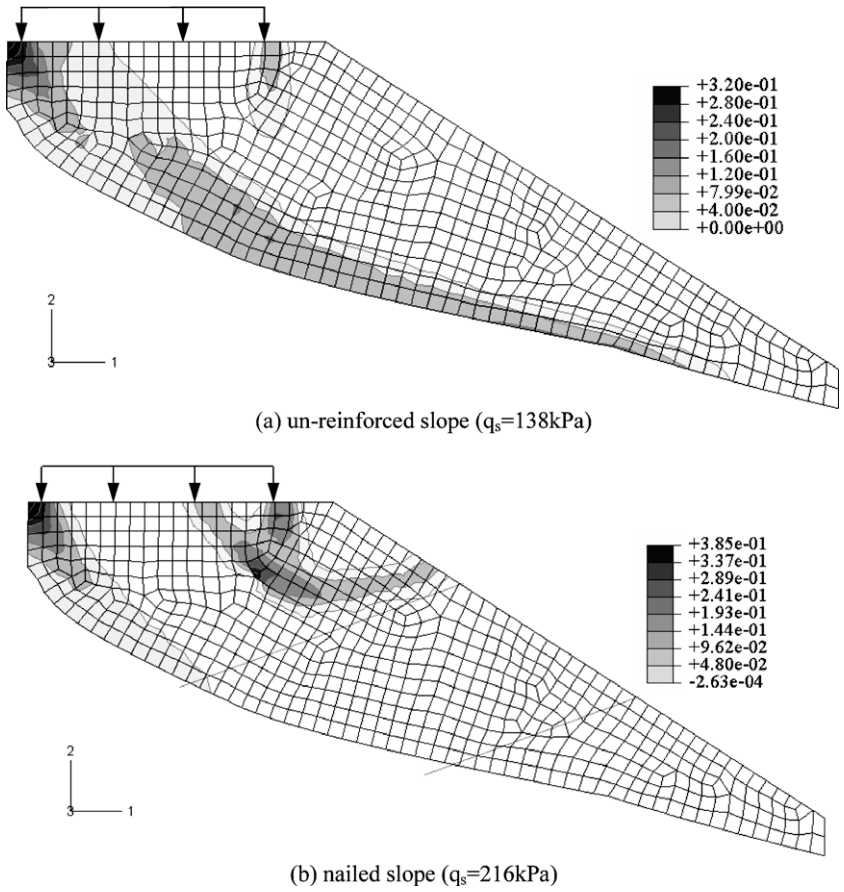

Fig. 14. Distribution of plastic shear strain in un-reinforced and nailed loose fill slopes at the onset of failure.

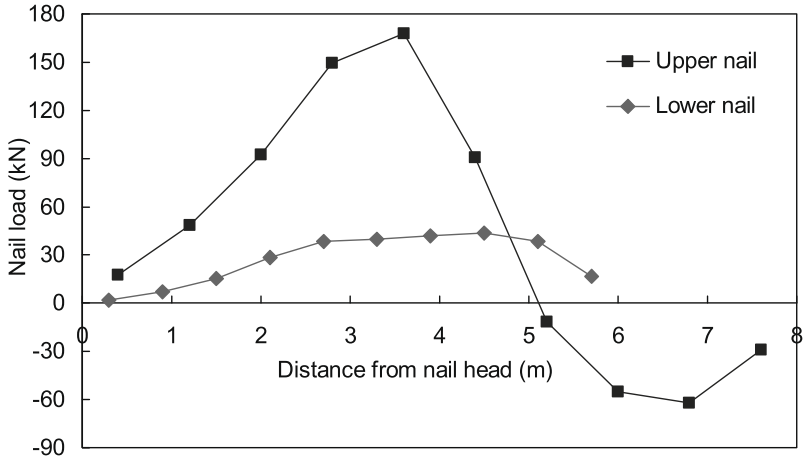

Fig. 15. Distribution of axial force in the nails at failure (q_s = 216 kPa).

was assumed to soften (due to static liquefaction) with its strength reduced to the critical state undrained shear resistance if the effective stress path intercepted the so-called collapse surface [23]. Their results illustrated that the mobilised nail forces were almost evenly distributed throughout the entire length of the soil nails. Tensile forces in the nails were mobilised by the movement of the facing structure due to the failure soil mass instead of by relative movement between the soil and the soil nails, since the interface friction was very small after liquefaction had occurred. Under this loading condition, the role of the facing structure becomes extremely important and the anchorage length of the nail into the in-situ ground needs to be long enough to effectively mobilise the nail forces. Although the assumptions made by Cheuk et al. [11] may have been too conservative, it is no doubt that the behaviour of a nailed loose fill slope can be very different under different types of loading conditions. The numerical model developed in the present study has proved to be a useful tool to shed light on the complex behaviour of soil nails in loose fill slopes.